

# A 2.5 T, 1.25 m Free Bore Superconducting Magnet for the Magnum-PSI Linear Plasma Generator

H. J. N. van Eck, H. H. J. ten Kate, A. V. Dudarev, T. Mulder, and A. Hervé

**Abstract**—DIFFER's main experiment Magnum-PSI is the only laboratory setup in the world capable of exposing materials to plasma conditions similar to those of future fusion reactors. The success of the Magnum-PSI experiment depends on the generation of a 2.5 T magnetic field without restricting the diagnostic access and operational aspects of the experiment.

This has been achieved with a magnet consisting of five superconducting solenoids wound on a 2.5 m long stainless steel coil former positioned in a cryostat offering a 1.25 m warm bore. A copper stabilized multifilamentary NbTi conductor with a 3.48 mm<sup>2</sup> cross section has been used, thus the magnet exhibits a total inductance of 500 H and a stored energy of 16 MJ. This presents quite a challenge for the protection scheme that has been implemented using a mix of back-to-back cold diodes and external dump resistors.

The coils generate a plateau shaped magnetic field adjustable up to 2.5 T while the distance between the coils allows for 16 room temperature view-ports. The coils are cooled with liquid helium using a re-condensing system operated with cryocoolers, while the magnet system cycles between zero and full field up to once per day. The magnetic stray field is shielded down to 1 mT outside the experimental area by iron walls that flank the magnet.

**Index Terms**—Fusion reactors, linear plasma generators, plasma-surface interaction, superconducting magnets.

## I. INTRODUCTION

The global endeavor of constructing ITER [1] [2] will result in the first reactor capable of creating and controlling a 'burning' plasma where the power generated by the fusion reactions will substantially exceed the external input power. After that a demonstration reactor, DEMO [3], is envisaged to be operational around 2050. The Fusion Energy research program at the Dutch Institute for Fundamental Energy Research (DIFFER) contributes to the development and validation of science and technology for the design and

operation of ITER and DEMO. The primary focus here is on one of the most critical aspects of fusion energy: the exhaust of heat and particles at the divertor [4].

DIFFER's main experiment Magnum-PSI [5]-[7] is capable of reproducing the heat and particle loading expected in the divertor region of future nuclear fusion reactors such as ITER and DEMO. Utilizing a wall stabilized arc plasma source [8], extremely high ion fluxes ( $> 10^{25} \text{ m}^{-2} \text{ s}^{-1}$ ) with heat fluxes of up to 50 MW m<sup>-2</sup>, can be achieved in steady state operation. A dedicated pulsed power supply is developed to investigate the effect of sudden energy eruptions from the nuclear fusion plasma (e.g. Edge Localized Modes) on the reactor wall materials, where heat loads up to 1 GW m<sup>-2</sup> can be achieved.

A key component to realize this is the superconducting magnet which provides constant magnetic fields up to 2.5 T. The axial magnetic field confines the high density, low temperature plasma produced by a cascaded arc into an intense magnetized plasma beam directed onto a target. This is required to enable extremely high cumulative plasma fluences for lifetime testing of wall materials, while at the same time not restricting the experiment excessively in terms of diagnostic access and operational aspects (e.g. ramp time, maintenance, magnetic shielding and running costs).

With a differentially pumped vacuum system, the neutral gas density in the target region can be maintained at a low level, despite the large quantities of neutral gas coming from the plasma source. This enables investigation of both attached-like and detached-like scenarios in high detail. Magnum-PSI has been designed to provide excellent optical access and has a large diagnostic suite, giving a well-defined set of plasma parameters and information on the retention of fuel species in the exposed material. The system is capable of handling large targets, up to an area of 0.12 x 0.6 m<sup>2</sup> and weight of 60 kg. The target holder is highly flexible and can be tilted to very low angles ( $< 3^\circ$ ), replicating the incidence angles of plasma onto the target material. These targets can be transported to the material analysis chamber without breaking vacuum to perform in situ ion beam analysis for extensive material characterization.

II. DESIGN

## II. DESIGN

### A. Requirements

After a conceptual design study [9] and subsequent detailed design, a superconducting magnet was built according to the following specifications:

1. A 1750 mm long plateau shaped magnetic field is generated between the exit of the source and the end of

Automatically generated dates of receipt and acceptance will be placed here; authors do not produce these dates. The work has been carried out within the framework of the EUROfusion Consortium and has received funding from the Euratom research and training programme 2014-2018 under grant agreement No 633053. The views and opinions expressed herein do not necessarily reflect those of the European Commission. DIFFER is a partner in the Trilateral Euregio Cluster TEC. DIFFER is part of the Netherlands Organisation for Scientific Research (NWO).

H. J. N. van Eck is with the Dutch Institute for Fundamental Energy Research (DIFFER), 5612 AJ Eindhoven, the Netherlands (e-mail: h.j.n.vaneck@diffier.nl).

H. H. J. ten Kate, A. V. Dudarev and T. Mulder are with CERN, Experimental Physics Department, Geneva, Switzerland.

A. Hervé is with the University of Wisconsin, Department of Physics, 1150 University Avenue, Madison, Wisconsin, USA.

the target plate by 5 NbTi superconducting solenoid coils. The coils are wound on one stainless steel coil former to sustain the large forces in a reliable and predictable way.

- The magnetic field strength is freely adjustable up to 2.5 T with a maximum deviation from the set point level (homogeneity) of 3% in the volume defined by  $-875 < z < 875$  mm and  $0 < r < 100$  mm. Here  $z$  is the coordinate along the magnetic axis of the solenoid,  $z = 0$  is the solenoid center.
- A 1250 mm free warm bore, supplemented with 16 radially distributed ports near the source and the target, guarantee good diagnostic access to the experiment. The axial distance between these radial access points is set by the dimensions of the experiment to 1250 mm.
- The magnetic field needs to be ramped up and down on a daily basis to allow for work to be done on diagnostics, the target and for general maintenance. In order to limit the impact on the experimental program to a minimum, while staying within reasonable technical demands, the time requirement for a ramp to full field is set to 30 minutes.
- The area directly outside the main experimental hall must be accessible to the general public and care has been taken to not exceed the exposure limits. From both practical and economic points of view, a passive shielding has been implemented by iron walls placed around the experiment.
- The coils are immersed in liquid helium and the evaporated helium is re-condensed by cryocoolers in a closed zero boil off system.

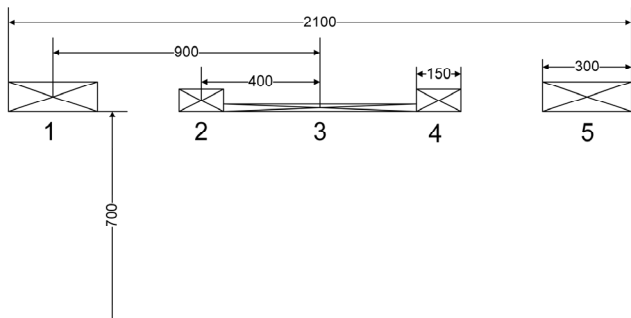


Fig. 1. Design of the basic coil system consisting of 5 solenoids wound on a single coil former. Rounded dimensions in mm.

### B. Coil system

The coil configuration is shown in Fig. 1 and the coil parameters are given in Table I. The spaces between coils 1 and 2 and between coils 4 and 5 are needed in order to fit the 174 mm diameter radial access ports. Coils 2 and 4 provide more windings at the ends of coil 3 to improve the homogeneity. The two outer coils have more layers of conductor to extend the length of the field plateau to 1750 mm. The coils are wound with 119 km of rectangular copper stabilized (Cu/Sc.: 8.7), multifilament NbTi conductor with a  $3.88 \text{ mm}^2$  insulated cross section. The flanges, in

between which the coils are wound, are 15 mm thick. Stiffening ribs keep the deformation of these flanges below 0.2 mm. The coils are connected in series and generate a plateau shaped field profile up to 2.5 T at an operating current of 257 A.

TABLE I  
COIL PARAMETERS

Coil	Number of layers	Windings per layer	Total number of windings	Wire length [km]
1	65	122	7930	38.3
2	42	62	2604	12.3
3	15	264	3960	18.1
4	42	62	2604	12.3
5	65	122	7930	38.3

### C. Protection circuit

For quench protection, a passive system has been chosen by subdividing the five coils into five electrical circuits (Fig. 2). Each circuit is shunted with a stack of cold diodes, with each diode connected to a copper heat sink of 793 grams. In the slow-dump configuration the external dump resistors can be used to slowly discharge the magnet in case of a power failure; in the fast-dump configuration they protect the cold diodes making sure that, after a quench, any current is removed rapidly from any circuit. Additionally, the coils are equipped with quench heaters which are automatically fired 10 seconds after the detection of a quench; the heaters are also hardwired to the emergency quench button.

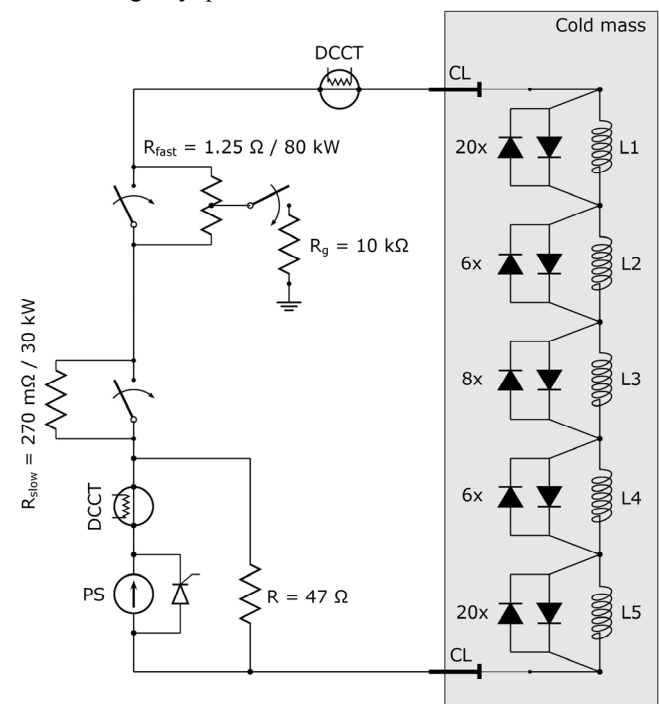


Fig. 2. Electrical diagram of the implemented protection scheme using a mix of back-to-back cold diodes and external dump resistors.

### D. Current leads

As the magnet needs to change field a few times per day, the power supply is connected to the coils via permanent

current leads. For this reason it is important to limit the heat conduction through the leads. This has been achieved by high temperature superconducting (HTS) current leads designed and manufactured by the ATLAS magnet group at CERN [10].

The HTS section comprises of 12 ReBCO tapes, a stainless-steel tube and two OFHC copper endpieces. The stainless-steel tube acts as a shunt for the ReBCO tapes in the case the HTS is in normal state and gives mechanical support. The stainless-steel tube in the HTS section is 160 mm long, it has an outer diameter of 18 mm and a wall thickness of 1 mm. The heat flow per lead to the magnet through the stainless steel tube is about 70 mW assuming 4 K and 60 K of the cold and warm tube ends respectively.

The ReBCO tapes are SCS4050 tapes made by SuperPower. The tapes have 20  $\mu\text{m}$  of copper stabilizer on each side, which implies a rather high heat flow to the 4 K stage. For this reason the copper stabilizing material is etched off the central part of the ReBCO tape to reduce the heat flow across the HTS section. The 12 tapes cause a heat flow of about 20 mW to the 4 K stage, increasing the total heat flow to the magnet to 90 mW. Each tape is able to carry some 275 A at 60 K and 150 mT parallel magnetic field. However, redundancy and a large safety margin is needed in the case a single or multiple tapes malfunction, 12 tapes are considered sufficient and allow operation at higher temperatures.

Two parallel NbTi/Cu LHC type 2 cables are soldered into the bottom copper joint and carry the current to the busbar of the magnet. These cables are flexible in all directions. One LHC cable is more than sufficient to carry the current to and from the busbar of the magnet. However, to ensure the superconducting state over the entire cable, a second LHC cable is added. The addition of the second LHC cable increases the heat flow to the busbar and thus decreases the temperature of the bottom copper joint. The effective copper section of the two cables is 25 mm<sup>2</sup>.

A flexible OFHC copper braid carries the current from the room temperature terminal to the top copper joint block. This braid is 30 mm wide, 3.5 mm thick and has an effective copper cross-section of 50 mm<sup>2</sup>. With a length of 680 mm the heat flow, per lead, to the top copper joint is 7 W without current and 13 W at operating current.

### E. Cryogenics

The magnet system was designed as a zero boil off system with two Sumitomo RDK-415D two stage cryocoolers and an additional Leybold Coolpower 250 MD one stage cryocooler connected to the radiation shield. The calculated main contributions to the heat loads on the two temperature levels (helium vessel and radiation shield) are given in Table II. With the chosen cooling configuration, the cooling capacity on the 4 K level during steady state operation ( $\sim 3$  W) is higher than the calculated heat load ( $\sim 2$  W). This excess power of roughly 1 W is used to re-condense the evaporated helium. Thermal calculations performed by the manufacturer show that the system should reach thermal equilibrium with an average radiation shield temperature of 60 K.

TABLE II  
CALCULATED HEAT LOSSES

	Heat load on shield at 60 K [W]	Heat load on 4 K level with shield at 60 K [W]
Radiation	88	1.11
Conduction	20	0.76
HTS current leads	26	0.18
<b>Total</b>	<b>134</b>	<b>2.05</b>

During charging or discharging, the changing magnetic field causes ac losses in the superconductor. These losses have been calculated to be  $\sim 10$  kJ for a 30 minute ramp from zero to full field. This leads to an additional evaporated helium loss of roughly 3000 l ( $\sim 4$  l liquid) which will be temporarily stored inside a 10 m<sup>3</sup> helium gas balloon. The helium gas balloon is flanged to the cryostat via a pipe system with filter, pump, heat exchanger, and regulated valves. The gas balloon is also equipped with the necessary safety devices (exhaust valve).

### F. Final design

Fig. 3 shows a drawing of the final design (left) as well as a cut-out (right) revealing the coils, helium vessel, radiation shield and vacuum vessel. The main magnet parameters are summarized in Table III.

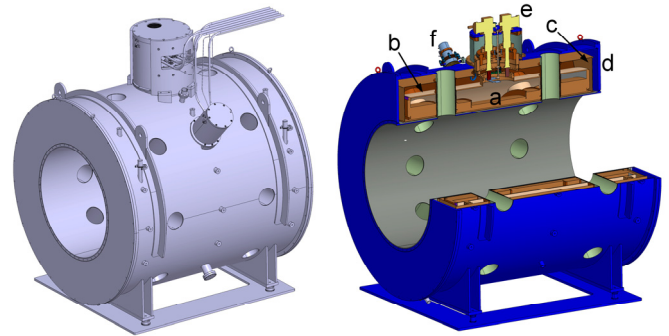


Fig. 3. Design drawing of the magnet system (left) as well as a cut-out (right) revealing the coils (a), helium vessel (b), radiation shield (c) and vacuum vessel (d). The turret (e) house two cryocoolers, while a third cryocooler (f) is connected to the radiation shield only.

TABLE III  
PARAMETERS OF THE MAGNET DESIGN

Room temperature bore [mm]	1250
Outer diameter [mm]	2400
Total length of the magnet system [mm]	2470
Number of coil sections [#]	5
Number of diagnostic ports [#]	16
Diameter of the radial ports [mm]	174
Magnetic field strength in centre region [T]	2.5
Homogeneity of the field in the plateau region [%]	$\sim 3$
Total weight [kg]	15000
Conductor length [km]	119
Operating current [A]	257
Engineering current density $J_e$ [A mm <sup>-2</sup> ]	66
Max. field on conductor [T]	4.84
Induction [H]	492.4
Stored energy [MJ]	16.3
Force on end coils [kN]	4023

### III. TEST RESULTS

The development of this magnet has been marked with many setbacks. During the first factory acceptance test (FAT) in 2010, the magnet showed erratic quench behavior. In total, the magnet quenched six times at varying currents. After inspection, it was found that some superconducting wires showed signs of movement and torsion due to incomplete clamping and insufficient stabilization. During the second FAT in 2011, the connection board and the outer layer of the coils were damaged by two electrical arcs due to weak points in the local insulation on one of the bus bars. As a result, it was decided to completely dismantle the coils and rewind them with new superconducting wire. The magnet was tested again in 2016 as described below.

#### A. Cryogenic situation

After cooldown it became clear that the final radiation shield temperature was higher than calculated. The shield reached an average temperature of about 80 K leading to a higher heat load on the 4 K level. Analysis showed that there is a bad connection between the shield cooler and the shield. The total heat load determined from the amount of evaporated helium gas and compensated for the 3 W cooling power of the cryocoolers, amounts to roughly 4 W.

The cryogenic situation was assessed and several solutions were discussed. The installation of a Cryomech HeRL45 reliquefier on top of the magnet was chosen to be the most robust and low risk solution. During the long-term stability test, the pressure of the helium vessel was controlled by the Cryomech controller operating the helium vessel heater. It was observed that the Cryomech heater was operating around 2 W, which means that the magnet system does require about 1 W of additional cooling capacity to remain in the zero boil off state. This value is very close to the heat load determined from the evaporated helium. The margin in capacity of about 2 W is now used to liquefy the helium gas after ramping.

#### B. Magnetic field profile

The on-axis magnetic field profile was measured with calibrated hall probes at a radial position of  $r = 100$  mm over a length of 1750 mm in steps of 50 mm over a full turn. The result is shown in Fig. 4. The measured deviation from the set point level falls within the specifications (< 3% deviation between  $-875$  mm  $< z < 875$  mm in a 200 mm diameter cylinder).

#### C. Maximum ramp speed

During the acceptance test it was observed that the magnet shows voltage oscillations whenever the current ramp rate was set above 3.5 A/min, and thus it was decided to limit the maximum ramp rate to this value. As a result, the ramp time from zero to full field is increased from 30 to 90 minutes. As a beneficial side effect, the amount of evaporated helium during ramping is decreased.

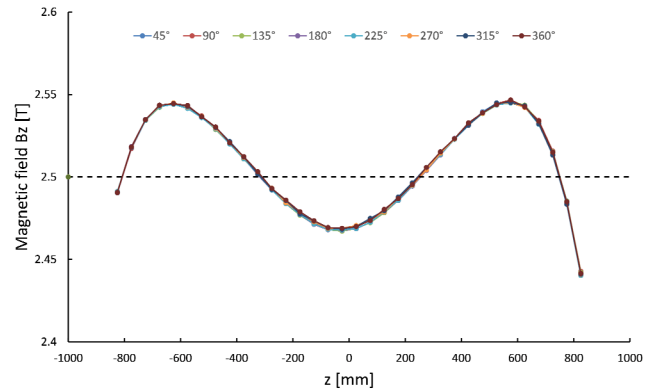


Fig. 4. Magnetic field profile at a radial position of  $r = 100$  mm as a function of  $z$  in steps of 50 mm by a full turn for an operational current of 257 A.

### IV. INSTALLATION ON SITE

#### A. Transport and installation

The magnet was transported to DIFFER during the night on a hydraulically cushioned extra low flatbed trailer. The magnet was lifted from the trailer by a 400-ton crane and moved through a hatch in the roof directly into the experimental hall. The magnet is placed on a trolley which can be transported over a rail system. In this way, the magnet is moved over the Magnum-PSI vacuum vessel.

#### B. Site acceptance test

After installation the magnet was cooled down and filled with liquid helium. The cryogenics system was taken into operation and its functionality was tested. The magnet was ramped up to 2.5 T three times. The cryogenic system was found to work properly, without needing the helium balloon due to the slower ramp rates that have to be used now. The magnetic field profile was almost identical to the one measured during the factory acceptance test.

### V. CONCLUSION

The installation of a 2.5 T superconducting magnet on the Magnum-PSI experiment has expanded the operational space to high fluence capabilities for the first time, making it possible to investigate the performance of materials during plasma exposures comparable to a sizable part of the ITER divertor lifetime. The experiment has shown its capability to reach conditions that enable fundamental studies of plasma-surface interactions in the regime relevant for fusion reactors such as ITER:  $10^{23} - 10^{25}$  m<sup>-2</sup> s<sup>-1</sup> hydrogen plasma flux densities at a temperature of 1-5 eV. This enables exploration of material evolution during a sizable part of their entire lifetime in ITER in the timespan of a couple of weeks. This capability makes the Magnum-PSI device truly unique.

#### ACKNOWLEDGMENT

The authors would like to thank D. Trompeter, J. Zeuschel, M. Pekeler, K. Schlenga and B. Prause for their support in making this project a success.

## REFERENCES

- [1] ITER Physics Basis, *Nucl. Fusion*, vol. 39, pp. 2137-2638, Dec. 1999.
- [2] K. Ikeda, "Progress in the ITER Physics Basis," *Nucl. Fusion*, vol. 47, no. 6, 2007.
- [3] G. Federici *et al.*, "Overview of the design approach and prioritization of R&D activities towards an EU DEMO," *Fusion Eng. Des.*, vol. 109-111, part B, pp. 1464-1474, Nov. 2016.
- [4] R. A. Pitts *et al.*, "A full tungsten divertor for ITER: Physics issues and design status," *J. Nucl. Mater.*, vol. 438, pp. S48-S56, Jul. 2013.
- [5] H. J. N. van Eck *et al.*, "Operational characteristics of the high flux plasma generator Magnum-PSI," *Fusion Eng. Des.*, vol. 89, pp. 2150-2154, May 2014.
- [6] S. Brezinsek *et al.*, *Nucl. Fusion*, vol. 57, no. 11, 116041, Nov. 2017.
- [7] Ch. Linsmeier *et al.*, *Nucl. Fusion*, vol. 57, no. 9, 092012, Sep. 2017.
- [8] M. C. M. van de Sanden *et al.*, "A combined Thomson-Rayleigh scattering diagnostic using an intensified photodiode array," *Rev. Sci. Instrum.*, vol. 63, no. 6, pp. 3369-3377, Jun. 1992.
- [9] H. J. N. van Eck *et al.*, "Pre-Design of the Superconducting Magnet System for Magnum-psi," *IEEE Trans. Appl. Supercond.*, vol. 16, no. 2, pp. 906-909, Jun. 2006.
- [10] T. Mulder, M. G. T. Mentink, A. Dudarev, H. F. P. Silva, and H. H. J. ten Kate, "Magnum-PSI current leads," CERN EDMS document 1838212, Jun. 2015.